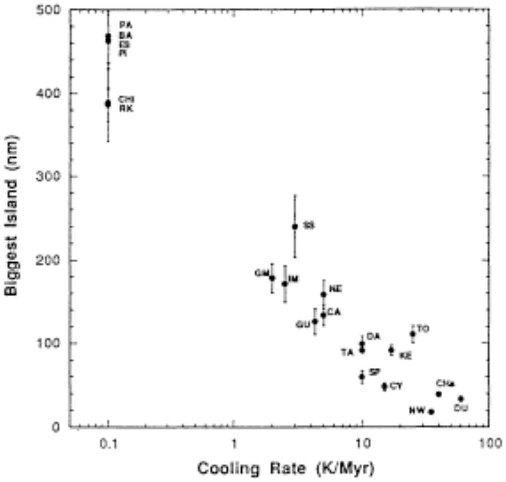

Fig. 1. The relationship between the size of the biggest island phase and the cooling rate of meteorites.

phase and the low-Ni honeycomb phase. The width of the island phase is governed by the cooling rate and Ni concentration. Since the Ni concentration is almost constant at the outermost region of the cloudy zone, only the cooling rate controls the size of the island phase. The purpose of this study is to further develop the relationship between the size of the island phase of the cloudy zone and the cooling rate of meteorites. The cloudy zone microstructure was studied using a JEOL 6300F high-resolution scanning electron microscope (HRSEM). The island phase size variation was measured using a Micro-Plan II image analysis system (DonSanto Co.). In this study, 21 meteorites including 6 mesosiderites [Patwar(PA), Barea(BA), Chinguetti(CHi), Pinnaroo(PI), Estherville(ES), RKPA 79015(RK)], 4 pallasites [Imilac(IM), Spearman(SP), Newport(NE), Glorieta Mountain(GM)], 8 iron meteorites [Tazewell-IIICD(TA), Duchene-IVA(DU), New Westville-IVA(NW), Dayton-IIICD(DA), Chinaulta-IVA(CHa), Toluca-IA(TO), Cape York-IIIA(CY), Carbo-IID(CA)], and 3 chondrites [Saint Severin-LL6(SS), Guarena-H6(GU), Kernouve-H6(KE)] were investigated.

Figure 1 shows the size variation of the island phase at the outermost region of the cloudy zone vs. the cooling rate of meteorites. The size of the biggest island phase clearly decreases with increasing cooling rate without regard to whether the host is an iron, stony-iron, or stony meteorite. The size of the biggest island phase varies approximately from 500 nm to 15 nm. Those meteorites that have cooled extremely fast (the IVA irons) have a very fine microstructure, which cannot be easily resolved even by employing a HRSEM. The metallographic cooling rates of the meteorites that we studied were taken from previous measurements [2–7]. Saikumar and Goldstein [6] have evaluated the methods to determine the cooling rates of iron meteorites considering impingement effects. They examined three iron meteorites that were included in this study, and showed that their measured cooling rates were greater by a factor of 5 compared to older cooling rates. The cooling-rate data from [3,4] were therefore multiplied by a factor of 5 for use in Fig. 1. Powell [5] suggested the cooling rate of 0.1 K/m.y. for mesosiderites. At this cooling rate, there appear to be two distinct size groups of mesosiderites: the first group with a width of the island phase about 460 nm including Patwar, Barea, Pinnaroo, and Estherville, and the second group with an approximately 390-nm size island phase including Chinguetti and RKPA79015. These data suggest that the mesosiderites may have varying cooling rates. In order to increase the accuracy of this new cooling rate method, the metallographic cooling rates of the meteorites will be recalculated using a revised computer program.

References: [1] Yang C. W. et al. (1993) *Meteoritics, 28,* 464. [2] Holland-Duffield C. E. et al. (1991) *Meteoritics, 26,* 97–103. [3] Goldstein J. I. and Short J. M. (1967) *GCA, 31,* 1001–1023. [4] Goldstein J. I. (1969) *Met. Res.,* 721–737. [5] Powell B. N. (1969) *GCA, 33,* 789–810. [6] Saikumar V. and Goldstein J. I. (1988) *GCA, 52,* 715–726. [7] Willis J. and Goldstein J. I. (1983) *Proc. LPSC 14th,* in *JGR, 88,* B287–B292.

CALCULATED STABILITY FIELD AND COMPOSITIONS OF NONIDEAL CONDENSATE LIQUIDS IN A SOLAR GAS.

S. Yoneda[1] and L. Grossman[1,2], [1]Department of the Geophysical Sciences and [2]Enrico Fermi Institute, The University of Chicago, Chicago IL 60637, USA.

Berman [1] derived an activity-composition model for $CaO-MgO-Al_2O_3-SiO_2$ (CMAS) liquids from thermodynamic data for minerals and pure oxide liquids calculated to fit known solid-solid reactions and liquidus relations for pure solid endmember components. The accuracy of this model can be assessed by comparing calculated and (observed) crystallization temperatures of phases from liquid CAIB [2]: spinel (Sp) 1819 (1823); melilite (Mel) 1717 (1673); anorthite (An) 1572 (1533); fassaite (Fass) 1542 (1503 K). In order to incorporate this liquid model into our condensation program [3], thermodynamic data for 33 solid phases used in [1] had to be substituted for data for the same phases used in [3] for consistency, despite our preference for data in [3]. Rerunning our condensation program at the total pressure (P^{tot}) $= 10^{-3}$ atm, where there are no stable liquids, using the modified data results in partial replacement of the hibonite field by $CaAl_2O_4$ and $CaAl_4O_7$, which delays the appearance of Mel by 35 K, but the condensation temperatures of all other species are within ± 6 K of those in [3].

CMAS liquids are stable in a solar gas at $P^{tot} \geq 5 \times 10^{-2}$ atm, a factor of 10 higher than estimated in [4]. At 5×10^{-2} atm, the liquid stability field is 10 K wide and the liquid coexists with forsterite (Fo) + Fass + Sp before crystallizing completely at 1556 K. The minimum pressure at which Fo and melt can coexist at equilibrium in a solar gas is thus more than a factor of 10^3 lower than predicted in [5], in which the colligative effects of additional components, in this case CaO and A_2O_3, were not considered.

At constant pressure, the changing composition of a solid condensate assemblage can cause melting to occur as the temperature falls. At $P^{tot} = 10^{-1}$ atm, the increasing Ak content of Mel with falling temperature causes the solidus temperature of the bulk composition of the perovskite (Pv) + Sp + Mel condensate assemblage to fall, causing melt to form from Mel and Sp at 1622 K, with all Mel dissolving in this melt at 1620 K. Because large amounts of MgO and SiO_2 condense from the gas into this melt, the bulk composition of the condensate assemblage changes from similar to that of a type A CAI to type B-like in this small temperature interval. At 1620 K, liquid is 77 wt% of the condensate, all Ca except that in Pv is in the liquid, Al is evenly distributed between liquid and Sp, the melt composition is C,M,A,S = 27, 15, 17, 41 wt%, and the bulk composition of the entire condensate assemblage is C,M,A,S = 22, 17, 28, 32 wt%. At 1617 K, the liquid becomes saturated in Fo and a large amount of this phase condenses from the gas. At 1594 K, Pv reacts with the liquid to form Fass, and the liquid is now 26 wt% of the condensate. At 1562 K, Sp begins to react with the liquid to form An + Fass + Fo, the liquid disappears at 1560 K, and Sp reacts completely with Fass to form An + Fo at 1557 K. The highly nonideal solution behavior of these liquids is illustrated by the last liquid to disappear, whose activity coefficients for C,M,A,S (l) are 6×10^{-5}, 0.02, 0.1, 0.4. Previous attempts to calculate stability fields of condensate liquids using ideal solution models [6,7] thus underestimate their stability considerably. At $P^{tot} = 1$ atm, condensation begins at higher T, with $CaAl_4O_7$ at 2020 K. This phase begins to melt at 1991 K to a liquid whose composition varies from C,M,A,S = 31, 0.1, 68, 1 to 32, 2, 43, 23 wt% at 1781 K where it freezes to Sp + Mel. Liquid reappears at 1760 K by melting of more Ak-rich Mel + Sp, and persists to 1526 K. At $P^{tot} = 10$ atm, liquid is the first condensate, persisting continuously from 2129 K to 1539 K, and Ca aluminates and Mel never form. We found similar effects by increasing the dust/gas ratio instead of the total pressure. Type C inclusions, thought by some to be liquid condensates [8], do not lie on the composition trajectory for either the liquid or the total condensate.

References: [1] Berman R. G. (1983) Ph.D. Thesis, Univ. of British Columbia. [2] Stolper E. (1982) *GCA, 46,* 2159. [3] Yoneda S. and Grossman L. (1994) *LPS XXV,* 1533. [4] Grossman L. and Clark S. P. Jr. (1973) *GCA, 37,* 635. [5] Wood J. A. (1963) *Icarus, 2,* 152. [6] Wagner R. D. and

Larimer J. W. (1978) *Meteoritics, 13,* 651; Wagner R. D. (1979) M.S. Thesis, Arizona State Univ. [7] Wood J. A. and Hashimoto A. (1993) *GCA, 57,* 2377. [8] Wark D. A. (1987) *GCA, 51,* 221.

ASTRONOMY BY MASS SPECTROMETRY: INTERSTELLAR GRAINS IN METEORITES.

E. Zinner, McDonnell Center for the Space Sciences and Physics Department, Washington University, One Brookings Drive, St. Louis MO 63130, USA.

Primitive meteorites contain small amounts of interstellar dust grains that survived the formation of the solar system [1,2]. Since these grains formed in stellar atmospheres, their study can provide information on nuclear and chemical processes in stars. To date, diamond, SiC, graphite, TiC, and corundum have been identified. Their circumstellar origin is indicated by their extremely anomalous isotopic compositions, originally of noble gases, but subsequently also of the major and refractory minor and trace elements.

While diamond and TiC are too small for single-grain analysis, SiC, graphite, and corundum range up to >1 µm in size and isotopic ratios can be measured for several elements by ion microprobe spectrometry [3–6]. The correlated isotopic data thus obtained set new constraints on theoretical models of nucleosynthesis and stellar evolution.

One type of information to be culled from isotopic measurements of interstellar grains is on the number of stellar sources that contributed material to the solar system. An example are inferences drawn from the Si and Ti isotopic compositions of individual SiC grains [4,7,8]. While there is strong evidence that most SiC grains must come from asymptotic giant branch (AGB) stars, the variations in Si and Ti isotopic ratios cannot be accounted for by nucleosynthetic processes within a single star and have been interpreted as being the result of several AGB stars with a range of metallicities [9]. Similarly, while corundum grains with large ^{17}O excesses and small to moderate ^{18}O depletions appear to have originated in red giant (RG) or AGB stars [6,10], the range of ^{16}O/^{18}O ratios can only be explained by multiple stellar sources with different metallicities [6].

Another type of information is obtained from single-grain isotopic data that either have no counterpart in astronomical observations or that cannot be explained by existing models of nucleosynthesis and thus provide stimulation for further theoretical work. An example are large ^{18}O depletions in corundum grains from Tieschitz [10]. No such depletions have been observed astronomically. Hot bottom burning (HBB) in intermediate mass AGB stars [11] is expected to result in large ^{18}O depletions but no detailed models exist that would relate the O isotopic compositions to ^{26}Al/^{27}Al ratios in stars with and without HBB. Another example are large ^{18}O excesses in graphite grains [12,13]. Many of these grains also have ^{15}N excesses, high ^{26}Al/^{27}Al ratios, ^{49}Ti excesses, and ^{28}Si excesses and deficits. A supernova origin of these grains is indicated by the large ^{18}O excesses predicted to exist in the outer layer of the ^{12}C-rich He-burning shell of massive stars. However, the details of correlated variations in the other elements are not understood yet and their explanation constitutes a challenge to nuclear astrophysics.

References: [1] Anders E. and Zinner E. (1993) *Meteoritics, 28,* 490–514. [2] Ott U. (1993) *Nature, 364,* 25–33. [3] Zinner E. et al. (1989) *GCA, 53,* 3273–3290. [4] Hoppe P. et al. (1994) *Astrophys. J.,* in press. [5] Amari S. et al. (1993) *Nature, 365,* 806–809. [6] Huss G. R. et al. (1994) *Astrophys. J.,* submitted. [7] Alexander C. M. O'D. (1993) *GCA, 57,* 2869–2888. [8] Stone J. et al. (1991) *EPSL, 107,* 570–581. [9] Gallino R. et al. (1994) *Astrophys. J.,* in press. [10] Nittler L. et al. (1994) *Nature,* submitted. [11] Renzini A. and Voli M. (1981) *Astron. Astrophys., 94,* 175–193. [12] Hoppe P. et al. (1992) *Meteoritics, 27,* 235. [13] Amari S. et al. (1994) *LPS XXV,* 27–28.

TRACE ELEMENTS OF OLIVINE IN SILICATE INCLUSIONS OF IAB IRON METEORITES REFLECTING LOW-TEMPERATURE HISTORY.

J. Zipfel[1], S. Weinbruch[2], S. Specht[1], and H. Palme[1], [1]Max-Planck-Institut für Chemie, 55020 Mainz, Germany, [2]Department of Material Sciences, Technical University Darmstadt, 64295 Darmstadt, Germany.

IAB iron meteorites with silicate inclusions may have formed at the core-mantle boundary of planetary bodies. Important constraints on the thermal evolution and the size of these bodies are given by cooling rates obtained from these meteorites. Recent metallographic cooling rates determined in metal grains enclosed in silicates of IAB irons are between 30° and 70 °C/m.y. [1]. An independent method for obtaining cooling rates of IAB silicate inclusions was suggested by [2]. The Ca contents of olivines are zoned from core to rim reflecting cooling from about 650° to 500°C, at similar temperatures as kamacite-taenite exsolution occurs. Calcium zoning of ol was observed in Landes [2], Caddo County [3], Woodbine, and Persimmon Creek (recent ion microprobe data). In addition, the central Ca content of olivine grains of different IAB meteorites should also reflect cooling rates. Olivine core compositions in silicates of several IAB meteorites, e.g., Persimmon Creek (PC), El Taco (ET), Woodbine (WB), Landes (LA), Caddo County (CC), and Copiapo (COP) were determined with the electron microprobe. This database (Table 1) allows us to (1) obtain a reasonable number for the highest core contents, (2) infer closure temperatures for Ca diffusion in olivine reflecting cooling rates, and (3) test for consistency between Ca-in-olivine and metallographic cooling rates.

All olivines have Ca contents below 140 ppm. The mean Ca core contents are decreasing from 132 ppm to 36 ppm in the order of CC > ET > PC > WB > LA comprising a temperature range of 650°–430°C. In Copiapo only a single grain with 141 ppm Ca was large enough for analysis. Calcium core contents are constant for CC, WB, and ET but variable for PC and LA. Olivine grains in three Landes thin sections have different mean Ca contents.

Generally, there is no correlation of Ca with grain size and/or Fa content. The constant central Ca in CC, ET, and WB olivines suggests equilibrium distribution of Ca between ol, cpx, and opx despite large variations in Fa contents of CC and ET. The highly variable Ca contents of LA olivine cores (22–114 ppm) require a different explanation. Perhaps Ca was lost during phosphate formation [4].

According to increasing metallographic cooling rates from LA, PC, to WB [1] and based on the concept of closure temperature one would expect a parallel increase in Ca core contents at similar grain sizes. This is, however, not observed.

TABLE 1. Calcium contents of olivine cores in silicates of IAB irons.

	(1)	(2)	Mean Ca (ppm)	Range of Ca (ppm)	Range of T °C
Persimmon Creek	5	10	96	64–128	542–629
El Taco	6	10	121	83–136	571–637
Woodbine	5	10	69	51–100	516–595
Landes					
(LAX)	5	5	58	47–74	505–557
(LAY)	6	5	75	38–114	483–612
(LA5)	5	5	36	22–53	437–519
Caddo County					
#1	6	5	132	117–146	615–647
#2	5	5	119	110–129	606–629
Copiapo	1	10	141		645

(1) Number of grains; (2) number of analyses within grain.

Nickel contents obtained by ion microprobe in LA ol and opx range from 4.3 to 5.1 ppm and from 1.8 to 3.3 ppm respectively. A single CC olivine has a Ni content of 3 ppm. These low Ni contents in olivine reflect equilibration temperatures of around 600°C. The use of Ca core contents and Ca profiles as indicators of low-temperature cooling rates requires further work. Nickel in ol may provide additional constraints on the thermal history.

References: [1] Herpfer M. A. et al. (1994) *GCA, 58,* 1353–1365. [2] Kohler T. et al. (1991) *N. Jb. Min. Mh., 9,* 423–431. [3] Zipfel J. et al. (1992) *Meteoritics, 27,* 312. [4] Eisenhour D. D. et al. (1993) *LPS XXIV,* 438–439.